Information and decoherence in a muon-fluorine coupled system

J. M. Wilkinson[1, *] and S. J. Blundell[1, †]
[1] *Clarendon Laboratory, University of Oxford Department of Physics,*
Parks Road, Oxford, OX1 3PJ, United Kingdom
(Dated: July 22, 2020)

The unitary evolution of a quantum system preserves its coherence, but interactions between the system and its environment result in decoherence, a process in which the quantum information stored in the system becomes degraded. A spin-polarized positively-charged muon implanted in a fluoride crystal realises such a coherent quantum system, and the entanglement of muon and nearest-neighbour fluorine nuclear spins gives rise to an oscillatory time-dependence of the muon polarization which can be detected and measured. Here we show that the decohering effect of more distant nuclear spins can be modelled quantitatively, allowing a very detailed description of the decoherence processes coupling the muon-fluorine 'system' with its 'environment', and allowing us to track the system entropy as the quantum information degrades. These results show how to precisely quantify the spin relaxation of muons implanted into quantum entangled states in fluoride crystals.

An important issue in the study of quantum mechanics is the interaction between a *system*, $\mathcal{S}$, considered as a few coupled quantum objects evolving in a manner described by some well-defined Hamiltonian, and its *environment*, $\mathcal{E}$, considered as a large bath consisting of many quantum objects. The action of the environment is to act as a source of decoherence [1] whereby quantum information, stored in the system and in principle readable from it, is degraded and leaks out into the environment where it can no longer be discovered. If the system and environment could be considered together as a single system, $\mathcal{S} \otimes \mathcal{E}$, this larger system would undergo unitary evolution and its von Neumann entropy, $S = -\mathrm{Tr}\rho \log_2 \rho$, where ρ is the density matrix of the $\mathcal{S} \otimes \mathcal{E}$ composite object, would be constant. However, we are rarely permitted this holistic view and are restricted to monitoring the reduced density matrix of the system, $\rho_{\mathcal{S}} = \mathrm{Tr}_{\mathcal{E}}\rho$, obtained by tracing out the degrees of freedom of the environment [2], and the entropy of $\mathcal{S}$ will tend to increase with time [3].

In order to study decoherence experimentally, it is necessary to identify well-defined scenarios in which the interaction between the system and environment is well characterised. One such scenario is provided by the dipolar interaction between a spin-polarized positively-charged muon μ^+ and the neighbouring nuclei in a fluoride compound, described by the Hamiltonian

$$\hat{\mathcal{H}} = \sum_{i>j} \frac{\mu_0 \gamma_i \gamma_j}{4\pi\hbar |\mathbf{r}_{ij}|^3} \Big[\mathbf{s}_i \cdot \mathbf{s}_j - 3\big(\mathbf{s}_i \cdot \hat{\mathbf{r}}_{ij}\big)\big(\mathbf{s}_j \cdot \hat{\mathbf{r}}_{ij}\big) \Big], \qquad (1)$$

where i and j label each nuclear spin and the muon, and $\mathbf{r}_{ij}$ is a vector linking spins $\mathbf{s}_i$ and $\mathbf{s}_j$, each with gyromagnetic ratios γ_i and γ_j respectively. Although other nuclei can give rise to coherent oscillations in muon spectra [4–6], fluorine nuclei are the best choice: they have spin $I = \frac{1}{2}$ with 100% abundance, and fluoride ions are very electronegative, making their surroundings particularly attractive sites for μ^+. Often a F–μ–F species forms after muon implantation, resulting in a distinctive oscillatory signal measured in the positron decay asymmetry [7], a direct result of the entanglement between the fluorine and muon spins [8]. The dipolar interaction between a single fluorine nuclear spin and a muon would result in the energy level spectrum shown in Fig. 1(a), while for two fluorine nuclear spins (the F–μ–F state), the spectrum is shown in Fig. 1(b). In both cases, the distinctive beating pattern of oscillations in the time-dependence of the muon polarization $P_z^{\mu}(t)$ occurs because of quantum interference between these energy eigenstates. This effect can be interpreted as a coherent exchange of spin polarization between the initially polarized muon and the initially unpolarized fluorine nuclei. These oscillations are shown in Fig. 1(c) and have been observed in numerous inorganic fluorides [7, 9, 10], fluoropolymers [11–13] and fluoride-containing molecular magnets [8]. However, good fits to the experimental data require multiplying the calculated coherent precession signals by a phenomenological relaxation function, often a stretched exponential, the parameters of which have no theoretical basis. A master equation approach could be used to model the non-unitary evolution of the reduced density matrix of the system [14], but this would still involve an arbitrary parameter quantifying the system-environment coupling. We will show below that an exact treatment is possible which includes the known couplings between the muon and more distant fluorine nuclei, thereby accurately modelling the *environment* of the F–μ–F *system*. These couplings result in a relaxation of the precession signal [solid line in Fig. 1(c)] that completely accounts for the data and makes contact with recent electronic structure calculations of the muon site [15, 16].

The effects of interactions with more distant fluorine nuclei can be understood by examining the energy eigenvalues shown in Fig. 1(d) where the eight next-nearest-neighbour (nnn) couplings that occur in the fluorite structure have also been included (analogous effects will

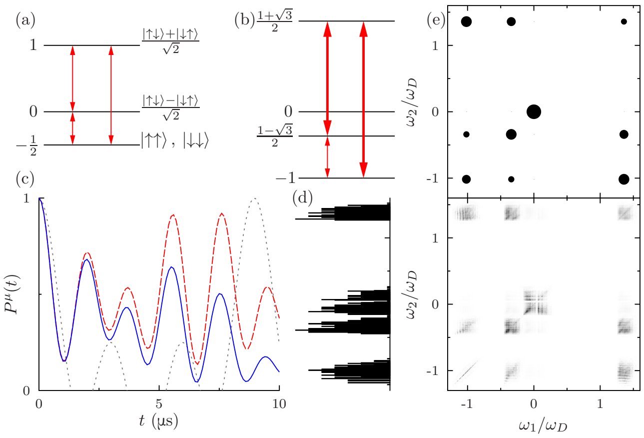

FIG. 1. (a) The energy levels in a F–μ coupled state. The eigenstates are labelled by the spins of the muon and the fluorine nucleus. The red arrows link levels between which quantum-mechanical interference can occur and the energies are in units of $\hbar\omega_{\rm D} = \hbar\mu_0\gamma_\mu\gamma_F/(4\pi r^3)$. (b) The energy levels for a F–μ–F state, also showing possible interefences (thicker lines connect energy levels between which there is the largest amplitude of quantum interference). The energy eigenvalues are very slightly different from those shown once the small F–F dipolar coupling is included, as will be done in all subsequent plots. (c) The time-dependence of the muon polarization $P^\mu(t)$ for isolated F–μ (dotted line), isolated F–μ–F (dashed line) and for F–μ–F also coupled to eight next-nearest-neighbour fluorine nuclear spins appropriate for the fluorite structure. These simulations are for an experiment in zero applied magnetic field, and assume a polycrystalline average over all possible orientations of the F–μ or F–μ–F species. (d) Energy levels for the F–μ–F state including next-nearest-neighbour fluorine nuclear spins. (e) Interefence amplitude for isolated F–μ–F (top panel) and with the next-nearest-neighbour couplings (bottom panel). The amplitude of the quantum interference between energy levels $\hbar\omega_1$ and $\hbar\omega_2$ is represented by the relative areas of the points in the top panel and by a grey scale in the bottom panel. The energy scales of (b) and (d) are lined up with these two panels.

occur in other fluoride crystal structures). The four energy levels in isolated F–μ–F are broadened by the nnn couplings into four bands of energy levels. The coherences between these energy levels are shown in the two-dimensional plots in Fig. 1(e), where the size of the point indicates the amplitude of the interference term between energy levels $\hbar\omega_1$ to $\hbar\omega_2$. These diagrams are reminiscent of two-dimensional NMR plots [17], but here there are no radiofrequency pulses and the interference between levels happen automatically in the unitary evolution of the quantum state. Thus, the overall structure for isolated F–μ–F in the upper panel is largely retained in the lower panel when including the more distant couplings, but a richer frequency spectrum results and this mixture of frequencies is responsible for the dephasing of the precession signal observed in experiments. ls -lr

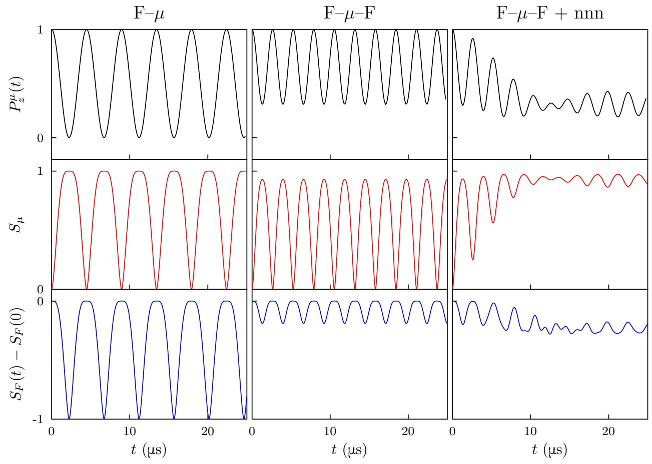

FIG. 2. von Neumann entropy for muon-fluorine states. The time-dependence of the muon polarization $P_z^\mu(t)$, the muon entropy S_μ (obtained by tracing out all the other spins), and the entropy of the entire fluorine system, S_F (note that $S_F(0) = N_F$, and our von Neumann entropies use $\log_2$, so that information is measured in bits. These are plotted for the three cases of isolated F–μ, isolated F–μ–F and environmentally decohering F–μ–F. These simulations assume the F–μ (or F–μ–F) bond is aligned with the initial muon spin polarization. (The other case is treated in [18] and shows similar behaviour.)

Further insight can be gained by calculating the time-dependence of the von Neumann entropy. We consider three cases: (i) the F–μ state; (ii) the F–μ–F state; and (iii) the F–μ–F state with eight nnn fluorine nuclei, appropriate for the fluorite structure [19]. The von Neumann entropy for these states remains constant at $S = N_F$ as the states evolve unitarily, where N_F is the number of fluorine nuclei in the cluster ($N_F = 1$, 2 and 10 for the three cases, respectively). This is because the implanted muon is initially spin-polarized and hence in a pure state, but the fluorine nuclei are initially unpolarized. By tracing out the fluorine or muon degrees of freedom, we are able to calculate the muon and fluorine reduced entropies, S_μ and S_F, as a function of time, see Fig. 2. The coupling between the muon and its fluoride environment results in the muon oscillating between being in a completely pure ($S_\mu = 0$) and mixed ($S_\mu > 0$) state, with the fluorine subsystem oscillating in antiphase. This can be interpreted in terms of quantum information exchanging back and forth between the muon and the fluorine subsystem; $P_z^\mu(t)$ reaches a maximum whenever information is stored on the muon and a minimum whenever it is residing in the fluoride subsystem. For F–μ, there are times when the muon is in a completely mixed state and the fluorine nucleus is in a completely pure state, but for F–μ–F the fluoride subsystem never evolves into a pure state. However, for both F–μ and F–μ–F, the muon periodically returns to a completely pure state ($S_\mu = 0$) and the quantum information is therefore never lost.

However, when the effect of the eight additional nnn fluorines is included, the muon never recovers to a pure state within the timescale of a typical muon experiment (25 µs). Thus the eight nnn fluorines act as a source of decoherence, so that information transferred from the muon remains in this subsystem and never completely returns to the muon [18]. This results in the oscillations in $P_z^\mu(t)$ exhibiting relaxation. However, even including nnn interactions only results in a larger interacting cluster and does not yet account for the decoherence due to the entire crystal, an issue we will return to.

To demonstrate how to account for system-environment interactions, we identified $\mathrm{CaF_2}$ as a model system since the Ca nuclear spin can be neglected (the most abundant Ca isotopes have $I = 0$ and make up 99.86% of the nuclei); thus only the fluorine nuclei contribute to the μSR spectrum. $\mathrm{CaF_2}$ adopts the cubic fluorite structure (lattice parameter $a = 5.451$ Å), and the muon site has been identified by density functional theory calculations (DFT+μ [15] using Quantum Espresso [20]). The muon site lies between two fluoride ions, each of which is pulled in towards the muon, resulting in a 14% reduction in the F–F separation distance. These calculations show that the effect of the muon on the positions of the more distant nuclei is negligible. We used an exact diagonalization method to evaluate the time evolution of the density matrix and simulate $P_z^\mu(t)$ [21, 22]. The muon enters the sample in a spin-polarized state, with the surrounding nuclei in mixed states and the time evolution of the muon's spin (labelled here as spin $i = 0$), $P^\mu(t)$, can be calculated as $P^\mu(t) = \dfrac{1}{2}\left\langle \mathrm{Tr}\left[\boldsymbol{\sigma}_{\hat{n}}^\mu \exp\left(\frac{-\mathrm{i}\hat{\mathcal{H}}t}{\hbar}\right)\boldsymbol{\sigma}_{\hat{n}}^\mu \exp\left(\frac{\mathrm{i}\hat{\mathcal{H}}t}{\hbar}\right)\right]\right\rangle_{\hat{n}}$, where $\langle\ldots\rangle_{\hat{n}}$ represents the angular average over $\hat{n}$ (appropriate for an experiment on a polycrystalline sample), and $\boldsymbol{\sigma}_{\hat{n}}^\mu$ is the Pauli spin operator for the muon in the direction of $\hat{n}$. An exact treatment has the virtue of accounting for all interactions precisely, but can only be carried out with a small number of nearest neighbours (as was performed in Ref. 22, albeit with a random-phase approximation to evaluate $P^\mu(t)$). The dimension of the Hilbert space is $2\prod_{i=1}^{M}(2I_i + 1)$, where the product is over the M nuclei included in the calculation (and the initial factor of two is due to the muon spin), and this dimension grows exponentially with M, making this method prohibitively computationally expensive when too many nuclei are included [23]. Hence we restrict our diagonalization method to include only nearest-neighbour and nnn fluorine nuclei, but scale the nnn interactions to account for all couplings in the infinite lattice. This can be done in a quantitative way by considering the second moment of the nuclear dipole field distribution, a quantity well known from the theory of broadening of NMR lines [24, 25]. The second moment σ_M^2 of this distribution at the muon site is given by $\sigma_M^2 = \frac{2}{3}(\frac{\mu_0}{4\pi})^2\hbar^2\gamma_\mu^2\sum_{j=1}^{M}\gamma_j^2 I_j(I_j+1)/r_j^6$, where r_j is the distance from the muon to the j^{th} nucleus with spin I_j and gyromagnetic ratio γ_j, $\gamma_\mu(= 2\pi \times 135.5$ MHz T^{-1}) is the muon gyromagnetic ratio, and the sum converges as $M \to \infty$. We then calculate ζ such that

$$\sigma_\infty^2 = \sigma_{\mathrm{nn}}^2 + \frac{2}{3}\Big(\frac{\mu_0}{4\pi}\Big)^2\hbar^2\gamma_\mu^2\sum_{j\in\mathrm{nnn}}\frac{\gamma_j^2 I_j(I_j+1)}{(\zeta r_j)^6}, \qquad (2)$$

where σ_{nn}^2 is due to nearest-neighbour couplings only and the sum is restricted to nnn. Thus we adjust our coupling to the nnn nuclei using the parameter ζ to mimic the effect of all more distant couplings. Because contributions to the second moment scale as $1/r_j^6$, we expect ζ to be close to unity (but $\zeta < 1$ because the more distant couplings make a positive contribution to σ_∞^2).

For $\mathrm{CaF_2}$, a direct calculation of equation (2) results in $\zeta = 0.943$, thus slightly enhancing the coupling with the nnn fluorine nuclei so that they are able to act as a proxy for all the coupling beyond the nnn fluorine to the rest of the lattice. The Hamiltonian can then be easily evaluated for this system of eleven particles (one muon, two nearest-neighbour fluorine nuclei and eight next-nearest-neighbour fluorine nuclei), and has dimension 2048×2048, whereas including the next shell of fluoride neighbours would become unfeasible for exact diagonalization. Our DFT+μ calculations on $\mathrm{CaF_2}$ show that the nnn fluoride ions do move towards the muon by a very small distance (approx 0.03 Å), and including this in our calculation of ζ leads to $\zeta = 0.937$.

We performed a μSR measurement on $\mathrm{CaF_2}$ and our measured asymmetry data on $\mathrm{CaF_2}$ were fitted to the function $A(t) = A_0 P^\mu(r_{\mathrm{nn}}, \zeta; t) + A_{\mathrm{bg}}$, where A_0 accounts for muons which form diamagnetic states, A_{bg} accounts for muons stopping outside the sample, and $P^\mu(r_{\mathrm{nn}}, \zeta; t)$ is the polarization signal on which we are focussing. (Here, r_{nn} corresponds to the nearest-neighbour F–μ distance, and ζ is the relative adjustment of the nnn coupling, defined in (2).) The value of A_0 is consistent with approximately 35% of muons implanting in diamagnetic states, suggesting the remainder are in muonium states, in agreement with previous work [26]. The agreement of our simulations with our experimentally observed $A(t)$ can be seen in Fig. 3(a). If only the nearest-neighbour fluorine nuclei are considered [isolated F–μ–F, dashed line in Fig. 3(a)] the fit is very poor, but the inclusion of nnn couplings results in an impressive agreement between theory and experiment [solid line in Fig. 3(a)]. Note that this fit does not need to include any phenomenological relaxation function of the sort used in previous studies [7–13]. Instead, the observed relaxation of the oscillations results entirely from the nnn couplings. Our fit uses only two fitting parameters, one of which is the distance between the muon and the two nearest-neighbour fluorine nuclei,

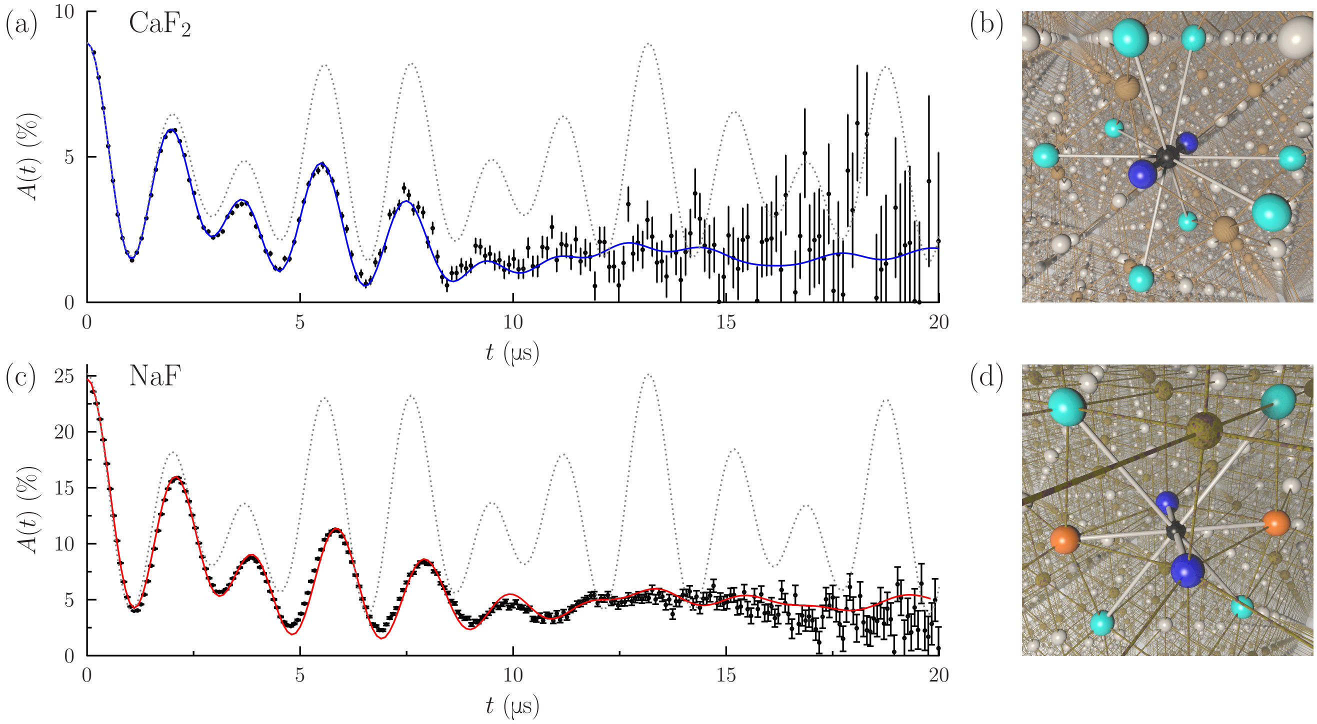

FIG. 3. (a) Muon decay asymmetry data $A(t)$ for polycrystalline CaF$_2$ (at 50 K), together with the simulated muon polarization without (dotted line) and with (solid line) the effects of environmental decoherence. (b) The muon (black sphere) strongly coupled to two fluorine nuclei (dark blue spheres), and weakly coupled to next-nearest neighbour fluorine nuclei (cyan spheres), embedded inside the fluorite structure of CaF$_2$. (c) $A(t)$ for NaF (at 100 K), with simulations as in (a). (d) The muon (black sphere) strongly coupled with the two nearest-neighbour fluorine nuclei (blue spheres, pulled close to the muon) and weakly coupled with the two nearest sodium nuclei (orange spheres, pushed away from the muon), and the next-nearest-neighbour fluorine nuclei (cyan spheres).

which is found to be 1.172(1) Å (very close to the DFT prediction of 1.134 Å, and dramatically shorter than the $\frac{a}{4} = 1.362$ Å expected if there was no muon-induced distortion). The second fitting parameter is $\zeta = 0.920(3)$, within 2% of our predicted value. These results demonstrate that, with suitable scaling, the eight nnn fluoride ions, which constitute a spin-subspace of dimensionality $2^8 = 256$, can provide an adequate representation of the full environment due to the entire crystal [Fig. 3(b)], allowing a quantitative description of the decoherence for this problem.

We also now demonstrate that this method can be extended to the more general case, in which the cation nuclear spin is non-negligible. NaF adopts the rocksalt structure and contains sodium nuclei which have spin $I = \frac{3}{2}$. In this case, the muon forms an F–μ–F state with the muon sitting at the centre of a square containing two fluorine ions and two sodium ions on the corners. The strongest coupling is with the two nearest fluorine nuclei, but the next largest couplings arise from the two sodium nuclei; the next largest couplings are due to four next-nearest-neighbour fluorine nuclei. We used the next-nearest-neighbour fluorine nuclei (subspace dimension 16) as a proxy for all of the more distant fluorine and sodium couplings, and evaluated the muon polarization function only for these nine spins [one muon, the two closest fluorines and sodiums, and four nnn fluorines, as shown in Fig. 3(d), giving a Hamiltonian with dimensionality 2048], and we also include the quadrupolar interaction of the Na nuclei in the electric field gradient of the muon [18]. We collected very high statistics μSR data on NaF so that we could carefully study the details of the precession signals. The fitting function used was $A(t) = A_0 P^{\mu}(r_{\mathrm{nn}}^{\mathrm{F}}, r_{\mathrm{nn}}^{\mathrm{Na}}, \zeta; t) + A_{\mathrm{bg}}$, and the analysis again demonstrated that the nearest-neighbour fluorine anions are pulled towards the muon and the sodium cations are pushed out (so that $r_{\mathrm{nn}}^{\mathrm{F}} = 1.1980(3)$ Å and $r_{\mathrm{nn}}^{\mathrm{Na}} = 2.31(3)$ Å, rather than both being 1.637 Å without the muon-induced distortion, values which are in good agreement with our DFT+μ calculations [18]). The value of $r_{\mathrm{nn}}^{\mathrm{Na}}$ was used in evaluating the quadrupole interaction via the calculated electric field gradient from the muon. The scaling parameter was fitted to be $\zeta = 0.86(1)$, very close to the calculated value $\zeta = 0.88$ [18]. The fit was in excellent agreement with data [Fig. 3(c)], and no phenomenological relaxation functions were required; all the parameters used in the fit are derived directly from the physics of the system.

In summary, we have found that the couplings between fluorine nuclei and positive muons can act as an ideal model system to observe the effects of quantum information dissipation through decoherence. We expect our method to find wide applicability in quantitatively describing decohering relaxation in muon experiments on a wide range of other crystalline materials.

We acknowledge support from EPSRC (grant code EP/N023803/1). Part of this work was carried out at the SFTC-ISIS muon facility, Rutherford Appleton Laboratory, UK and we thank P. Biswas, F. L. Pratt and P. J. Baker for assistance. The DFT+μ and entropy calculations were performed on the ARC HPC facility at the University of Oxford. The μSR data on CaF_2 will be made available on doi:10.5286/ISIS.E.RB1990125, and the NaF data will be available on doi:10.5286/ISIS.E.RB2010203-1.

---

* john.wilkinson@physics.ox.ac.uk
† stephen.blundell@physics.ox.ac.uk

[1] W. H. Zurek, Rev. Mod. Phys. **75**, 715 (2003)
[2] E. Joos and H. D. Zeh, Z. Phys. B **59**, 223 (1985)
[3] V. Vedral, Rev. Mod. Phys. **74**, 197 (2002)
[4] A. Schenck and K. M. Crowe, Phys. Rev. Lett. **26**, 57 (1971)
[5] J.S. Lord, S.P. Cottrell and W.G. Williams, Physica B **289–290**, 495 (2000)
[6] P. Mendels, F. Bert, M. A. de Vries, A. Olariu, A. Harrison, F. Duc, J. C. Trombe, J. S. Lord, A. Amato, and C. Baines, Phys. Rev. Lett. **98**, 077204 (2007)
[7] J. H. Brewer, S. R. Kreitzman, D. R. Noakes, E. J. Ansaldo, D. R. Harshman and R. Keitel, Phys. Rev. B **33**, 7813 (1986)
[8] T. Lancaster, S. J. Blundell, P. J. Baker, M. L. Brooks, W. Hayes, F. L. Pratt, J. L. Manson, M. M. Conner and J. A. Schlueter, Phys. Rev. Lett. **99**, 267601 (2007) Phys. Rev. Lett. **99**, 267601 (2007).
[9] D. R. Noakes, E. J. Ansaldo, S. R. Kreitzman, and G. M. Luke, J. Phys. Chem. Sol. **54**, 785–792 (1993).
[10] T. Lancaster, S. J. Blundell, P. J. Baker, W. Hayes, S. R. Giblin, S. E. McLain, F. L. Pratt, Z. Salman, E. A. Jacobs, J. F. C. Turner and T. Barnes, Phys. Rev. B **75**, 220408(R) (2007)
[11] F. L. Pratt, S. J. Blundell, I. M. Marshall, T. Lancaster, A. Husmann, C. Steer, W. Hayes, C. Fischmeister, R. E. Martin and A. B. Holmes, Physica B **326**, 34 (2003)
[12] K. Nishiyama, S. W. Nishiyama and W. Higemoto, Physica B **326**, 41 (2003).
[13] T. Lancaster, F. L. Pratt, S. J. Blundell, I. McKenzie and H. E. Assender, J. Phys.: Condens. Matter **21**, 346004 (2009).
[14] G. Lindblad, Commun. Math. Phys. **48**, 119–130 (1976).
[15] J. S. Möller, D. Ceresoli, T. Lancaster, N. Marzari and S. J. Blundell, Phys. Rev. B **87**, 121108(R) (2013).
[16] F. Bernardini, P. Bonfá, S. Massidda and R. De Renzi, Phys. Rev. B **87**, 115148 (2013).
[17] W. P. Aue, E. Bartholdi and R. R. Ernst, J. Chem. Phys. **64** 2229 (1976).
[18] Further calculations and experimental details are available in the Supplemental Material, which includes Refs. 27 and 28.
[19] W. Hayes (editor) *Crystals with the fluorite structure*, Oxford Univ. Press (1974).
[20] P. Giannozzi et al. J. Phys.: Condens. Matter **21**, 395502 (2009).
[21] E. Roduner and H. Fischer, Chem. Phys. Lett. **65**, 582 (1979).
[22] M. Celio, Phys. Rev. Lett. **56**, 2720 (1986).
[23] Earlier attempts to include coupling beyond the nearest-neighbour fluorines using the method in Ref. 22 were carried out, but were somewhat limited by the computing power then available; see J. H. Brewer, D. R. Harshman, R. Keitel, S. R. Kreitzman, G. M. Luke, D. R. Noakes, R. E. Turner and E. J. Ansaldo, Hyp. Int. **32**, 677 (1986) and D. R. Harshman and M. Celio, Hyp. Int. **32**, 683 (1986).
[24] J. H. Van Vleck, Phys. Rev. **74**, 1168-1183 (1948).
[25] A. Abragam, A. *The Principles of Nuclear Magnetism* Oxford Univ. Press, London, (1961).
[26] R. F. Kiefl, E. Holzschuh, H. Keller, W. Kundig, P. F. Meier, B. D. Patterson, J. W. Schneider, K. W. Blazey, S. L. Rudaz and A. B. Denison, Phys. Rev. Lett. **53**, 90 (1984).
[27] S. F. J. Cox, J. Phys. C: Solid State Phys. **20**, 3187 (1987).
[28] E. Roduner and H. Fischer, Chem. Phys. **54**, 261 (1981).